International Journal of General Medicine

Dovepress

open access to scientific and medical research

Open Access Full Text Article

ORIGINAL RESEARCH

Prognostic and Immunological Roles of CES2 in Breast Cancer and Potential Application of CES2-Targeted Fluorescent Probe DDAB in Breast Surgery

Weikun Qu[1,2,*], Yalu Yao[1,*], Yaqian Liu[1,*], HyonSu Jo[1,3], Qianran Zhang[1,*], Haidong Zhao[1,*]

[1]Department of Oncology & Department of Breast Surgery, The Second Hospital of Dalian Medical University, Dalian, 116023, People's Republic of China; [2]OPO Office, The Second Hospital of Dalian Medical University, Dalian, 116023, People's Republic of China; [3]Department of General Surgery, the Hospital of Pyongyang Medical University, Pyongyang, 999093, Democratic People's Republic of Korea

*These authors contributed equally to this work

Correspondence: Haidong Zhao; Qianran Zhang, Department of Breast Surgery, Second Affiliated Hospital of Dalian Medical University, 467, Zhongshan Road, Shahekou District, Dalian, Liaoning, 116023, People's Republic of China, Tel +86 13354288881; +86 13278089966, Email z.hddl@hotmail.com; 382026591@qq.com

Purpose: The expression and function of CES2 in breast cancer (BRCA) has not been fully elucidated. The purpose of this study was to investigate its clinical significance in BRCA.

Patients and Methods: Bioinformatics analysis tools and databases, including The Cancer Genome Atlas (TCGA), Gene Expression Omnibus (GEO) databases, SURVIVAL packages, STRING database, Gene Ontology (GO) enrichment, Kyoto Encyclopedia of Genes and Genomes (KEGG) pathway analysis, Gene set variation analysis (GSVA), and Tumor Immunity Estimation Resource (TIMER), were utilized to measure the expression level and clarify the clinical significance of CES2 in BRCA. In addition, we verified the expression level of CES2 in BRCA at the cellular and tissue levels by Western blot, immunohistochemistry (IHC) and real-time fluorescence quantitative PCR assays. Furthermore, DDAB is the first reported near-infrared fluorescent probe that can be used to monitor CES2 in vivo. We applied the CES2-targeted fluorescent probe DDAB in BRCA for the first time and verified its physicochemical properties and labeling sorting ability by CCK-8, cytofluorimetric imaging, flow cytometry fluorescence detection, and isolated human tumor tissue imaging assays.

Results: The expression of CES2 was higher in normal tissues than that in BRCA tissues. Patients with lower CES2 expression in the BRCA T4 stage had a poorer prognosis. Finally, we applied the CES2-targeted fluorescent probe DDAB in BRCA for the first time, which was demonstrated to have good cellular imaging performance with low biological toxicity in BRCA cells and ex vivo human breast tumor tissue models.

Conclusion: CES2 can be considered a potential biomarker to predict the prognosis of breast cancer at stage T4 and might contribute to the development of immunological treatment strategies. Meanwhile, CES2 is able to distinguish between breast normal and tumor tissues, the CES2-targeting NIR fluorescent probe DDAB may have potential for surgical applications in BRCA.

Keywords: carboxylesterase 2, breast cancer, fluorescent probe, bioinformatics, molecular markers

Introduction

According to statistics, the incidence of breast cancer (BRCA) surpassed that of lung cancer as the world's leading cancer in 2020, with approximately 2.3 million new cases accounting for 11.7% of all cancer cases.[1]

Approximately 70–80% of patients with early-stage non-metastatic BRCA can be cured with available treatments, whereas patients with advanced-stage BRCA with distant metastases cannot.[2] Screening and diagnosis of early BRCA are indispensable, and are particularly crucial to reduce patient morbidity and mortality.[3,4] A variety of gene expression

Received: 2 February 2023
Accepted: 17 April 2023
Published: 27 April 2023

changes are known to contribute to the development of BRCA. However, there is still a lack of research on the key genes that contribute to the develop.

Carboxylesterases (CES1 and CES2) are the two most prominent classes of carboxylesterases (CESs) in the human body.[5] As key enzymes in the serine hydrolase superfamily, researchers have found that they play a crucial role in the metabolism of endogenous esters, ester-containing drugs, and environmental toxins.[6–9] Serine hydrolase carboxylesterase 2 (CES2) plays an important role in the metabolic activation of various anticancer drugs such as irinotecan and gemcitabine.[10–12] In recent years, with a focus on the role of CES2 in cancer development, studies have shown that high expression of CES2 in tumor cells is a prognostic indicator of poor overall survival in metastatic colorectal cancer and neuroblastoma patients who do not respond to chemotherapy.[13,14] A recent study has shown that CES2 maintains HNF4α expression through an epoxide hydrolase-dependent regulatory loop to promote pancreatic cancer progression.[15] However, whether CES2 has potential as a prognostic biomarker for BRCA is not yet known. Therefore, it is important to elucidate the expression of CES2 in BRCA and its potential prognostic value.

In this experiment, we also used the CES2-targeted fluorescent probe DDAB, a DDAO-based near-infrared fluorescent probe. DDAO was chosen as the basic fluorophore because of its desirable spectral properties, good photostability, low toxicity, and feasibility for structural modification.[16] DDAB is the first reported NIR fluorescent probe that can be used to monitor CES2 in vivo for the selective and sensitive detection of CES2 in complex biological samples. It emits in the NIR region to rapidly turn on the fluorescence response, with rapid targeting and specificity for CES2, and has strong deep tissue penetration. In addition, DDAB can penetrate cell membranes and is suitable for the detection of CES2 in living cells, tissues, and organs such as the mouse liver.[16] We further aimed to explore the physicochemical properties and biological applications of DDAB fluorescent probes in BRCA.

In summary, given the important role of CES2 in tumorigenesis and progression, this study aimed to investigate the prognostic value of CES2 and its correlation with BRCA immune infiltration. In addition, we identified the potential of the CES2-targeted fluorescent probe DDAB for use in breast cancer surgery.

Materials and Methods

Comparison of CES2 Expression Levels

Data from The Cancer Genome Atlas (TCGA) database were used to analyze CES2 expression in 30 types of human cancers, 1109 invasive BRCA tissues and 113 normal breast tissues, and 113 invasive BRCA tissues and their paired adjacent normal breast tissues. The expression of CES2 in different estrogen receptor (ER), progesterone receptor (PR), human epidermal growth factor receptor 2 (HER2) statuses, and different PAM50 types was analyzed simultaneously based on the TCGA database. In addition, the gene expression profiles GSE45827 and GSE65194 were extracted from the Gene Expression Omnibus (GEO) database to analyze the expression of CES2.

Correlation Analysis of CES2 with Prognosis and Diagnosis

Kaplan–Meier plots were created and validated using the SURVIVAL package for survival analysis. The diagnostic value of CES2 in patients with BRCA was assessed using ROC curves, analyzed with the pROC package, and visualized with ggplot2.

PPI Network Construction and Functional Enrichment Analysis

We constructed a PPI network for CES2 using the Search Tool for Interacting Genes/Proteins (STRING) database to explore CES2-associated proteins. We then analyzed the predicted pathways of CES2 and its associated proteins using GO and KEGG.

Correlation Analysis of Immune Cell Infiltration

We used the TIMER and single-sample gene set enrichment analysis (ssGSEA) to assess the relationship between CES2 and tumor purity as well as several immune cells, including B cells, neutrophils, macrophages, CD4+ T cells, and CD8+ T cells. Spearman correlation analysis was used to investigate the correlation between CES2 levels and immune cell infiltration.

Patient Samples

Postoperative pathological tissues with confirmed BRCA at the Second Hospital of Dalian Medical University were randomly selected to verify the expression of CES2 in BRCA tissues. The Ethics Committee of the Second Hospital of Dalian Medical University approved this study in strict accordance with the Declaration of Helsinki (No.2022065). Written informed consent was obtained from all the patients.

Cell Culture

Human normal breast epithelial cells (MCF-10A) and BRCA cell lines (MCF-7, MDA-MB-231, MDA-MB-468, HCC1954, HCC38, SK-BR3, and T47D) were obtained from American Typical Culture Collection (ATCC, Manassas, VA). Normal breast MCF-10A cells were cultured in a mammary epithelium-specific medium (Lonza). MDA-MB-231 and MDA-MB-468 cells were cultured in sealed medium containing L-15 basal medium (Solarbio). MCF-7 cells were cultured in DMEM medium (Gibco). HCC1954, HCC38, SK-BR3, and T47D cells were cultured in 1640 medium (Gibco). In addition to the above dedicated medium, the addition of 10% fetal bovine serum (VivaCell) was essential, while penicillin/streptomycin (Hyclone) was selectively added according to the cell status. Growth conditions for all cells were 37°C and 5% CO_2 concentration.

RNA Extraction and Real-Time Quantitative PCR

Total RNA was extracted from the cultured cells using RNAiso Plus (TaKaRa). Reverse transcription was performed using the PrimeScript RT reagent kit with gDNA Eraser (TaKaRa). RT-qPCR was performed using TB Green Premix EX Tag II (TaKaRa), according to the manufacturer's instructions. Primers were as follows: GAPDH, forward (F): 5'-ACGAGTGTGTCTTCGCTTGT-3', reverse (R): 5'-TCTTTACTCTTGCCCCGCAG-3'; CES2, forward (F): 5'-GCACCGTCAAGGCTGAGAAC-3', reverse (R): 5'-TGGTGAAGACGCCAGTGGA-3'.

Western Blotting

Proteins were isolated from the cultured cells using SDS lysis buffer containing freshly added protease inhibitors. Quantitative analysis of the protein content was performed using a BCA kit (Tiangen) and separated by 10% sodium dodecyl sulfate-polyacrylamide gel electrophoresis. The separated proteins were transferred to nitrocellulose membranes and incubated with 5% skim milk. The membranes were incubated overnight at 4°C with primary antibodies, including CES2 (antibody DF6433, Affinity), GAPDH (antibody WL01114, Wanleibio). After washing, the membranes were incubated with fluorophore-coupled secondary antibodies (Li-COR). Protein band images were captured using the ODYSSEY IR imaging system. The antibody dilution ratios were as follows: rabbit anti-CES2 antibody, 1:1000; rabbit anti-GAPDH antibody, 1:3000; and fluorescent rabbit secondary antibody, 1:15,000.

Immunohistochemistry (IHC)

Human breast tissues were fixed in 10% formalin overnight and then embedded in paraffin. Next, the tissue sections were dewaxed, rehydrated, and treated in citrate buffer and 3% hydrogen peroxide, respectively. And then incubated overnight at 4°C with anti- CES2 (antibody DF6433, 1:100, Affinity). The bound antibodies were detected using Secondary antibody binding to horseradish peroxidase and developed with 3,3'-diaminobenzidine using a two-step test kit (PV-9000, Zhongshan Jinqiao Biological).

CCK-8 Experiment

Cells with confirmed concentrations were re-inoculated uniformly in 96-well plates at a density of 8.0×10^3/well and cultured. The fluorescent probe solution reconstituted with complete medium at different concentration gradients (0 μM, 0.1 μM, 1 μM, 5 μM, 10 μM, and 20 μM) was added back to the 96-well plate at 200 μL/well for approximately 24 hours under light-proof conditions, while three parallel wells were set up with different concentration gradient solutions as well as a blank control group, and then placed in an incubator to allow the probe and cells to act together incubation. After the probes acted on the cells for 24 and 48 hours, respectively, we configured the CCK-8 detection reagent (Bimake) under light-proof conditions to detect the absorbance between different wells.

Cell Fluorescence Imaging Experiment

Cells with confirmed concentrations were inoculated uniformly at a density of 2.5×10^4 in small 30 mm laser confocal imaging dishes and cultured. After the cells had completely adhered to the wall, the DDAB probe master mix was diluted with PBS reagent, added to the culture dishes under light-proof conditions to obtain a final concentration of 2 μM, and placed in the incubator for 30 min. After incubation, the cells were placed directly under the NIR two-color laser imager, and the excitation light was set to 700 nm to compare and count the fluorescence values of the imaging of human normal breast cells and BRCA cells.

Flow Cytometry Fluorescence Detection Assay

In MCF-10A normal breast cells and MCF7, HCC1954, MDA-MB-231, HCC1937, and other BRCA cells, 500 μL PBS reagent was added to prepare cell suspensions, while DDAB probes were added to each group of cells in the corresponding experimental groups under light-proof conditions, so that the final concentration of the probes was 5 μM. To prevent cell clumps from clogging the flow cytometer, each sample was filtered with a nylon membrane, and approximately 10^5 cells at a time were detected by flow cytometer aspiration (excitation wavelength of 700 nm), and the number of cells labeled by fluorescence was compared and counted.

Human ex vivo Tumor Tissue Imaging Experiment

Hospital clinical ethical approval certificates were obtained before the experiment. After modified radical mastectomy for BRCA, a patient's isolated BRCA tissue and normal tissues adjacent to the cancer were taken, and the volume of the tissue block was approximately 2×2 × 1 cm; the surfaces of both tissues were evenly coated with 200 μM DDAB probe-PBS buffer solution, and left for 5 min at 37 °C and protected from light. The difference in fluorescence intensity between the normal and paracancerous tissues was compared using a handheld near-infrared fluorescence imager.

Statistical Analysis

Most of the data statistics for this study were performed in the XIANTAO platform (https://www.xiantao.love/). Statistical significance was set at $P < 0.05$. We analyzed the data using the R software (v.3.6.3). Both the chi-square test and Fisher's exact test were used to analyze the clinical information. In addition, the Wilcoxon rank-sum test was used. All the experiment statistical analyses were performed using the GraphPad Prism 8.0 software package and presented as mean± standard deviation (SD). Statistical significance was described as follows: *$P < 0.05$; **$P < 0.01$; ***$P < 0.001$; ****$P < 0.0001$.

Results

Characterization of Clinical Information of BRCA Patients Based on TCGA

The clinical history of 1222 patients was obtained from the TCGA database, including race, histological typing, PAM50 typing, PR expression, and estrogen receptor (ER) expression status. Detailed information is presented in Table 1, and clinical information was calculated using data filtering.

Reduced Expression of CES2 in BRCA

Differential expression of CES2 was analyzed in 30 pan-cancer tissues. We observed that CES2 expression levels were higher in tumor tissues from 10 types of cancer and lower in tumor tissues from 14 types of cancer. Compared to normal tissue, Low CES2 expression in BRCA tissues was observed in both paired and unpaired comparative studies based on TCGA database ($p < 0.001$). Correlation analysis revealed statistically significant differences in CES2 expression levels across PR, ER, HER2 status, and PAM50 typing (Figure 1A–G). CES2 expression levels in BRCA were validated in GSE45827 and GSE65194 ($P < 0.001$) (Figure 1H and I).

Table 1 Clinical Characteristics Analysis of Patients with Invasive Breast Cancer Based on TCGA

Characteristic	Low Expression of CES2	High Expression of CES2	*p*
n	541	542	
T stage, n (%)			0.139
T1	126 (11.7%)	151 (14%)	
T2	333 (30.8%)	296 (27.4%)	
T3	66 (6.1%)	73 (6.8%)	
T4	15 (1.4%)	20 (1.9%)	
N stage, n (%)			0.27
N0	272 (25.6%)	242 (22.7%)	
N1	171 (16.1%)	187 (17.6%)	
N2	56 (5.3%)	60 (5.6%)	
N3	33 (3.1%)	43 (4%)	
M stage, n (%)			0.473
M0	457 (49.6%)	445 (48.3%)	
M1	8 (0.9%)	12 (1.3%)	
Pathologic stage, n (%)			0.055
Stage I	85 (8%)	96 (9.1%)	
Stage II	332 (31.3%)	287 (27.1%)	
Stage III	108 (10.2%)	134 (12.6%)	
Stage IV	7 (0.7%)	11 (1%)	
Race, n (%)			0.003
Asian	38 (3.8%)	22 (2.2%)	
Black or African American	104 (10.5%)	77 (7.7%)	
White	352 (35.4%)	401 (40.3%)	
Age, n (%)			0.257
<=60	310 (28.6%)	291 (26.9%)	
>60	231 (21.3%)	251 (23.2%)	
Histological type, n (%)			0.014
Infiltrating Ductal Carcinoma	408 (41.8%)	364 (37.3%)	
Infiltrating Lobular Carcinoma	88 (9%)	117 (12%)	
PR status, n (%)			< 0.001
Negative	212 (20.5%)	130 (12.6%)	
Indeterminate	1 (0.1%)	3 (0.3%)	
Positive	301 (29.1%)	387 (37.4%)	

(*Continued*)

Table 1 (Continued).

Characteristic	Low Expression of CES2	High Expression of CES2	*p*
ER status, n (%)			< 0.001
Negative	164 (15.8%)	76 (7.3%)	
Indeterminate	0 (0%)	2 (0.2%)	
Positive	351 (33.9%)	442 (42.7%)	
HER2 status, n (%)			0.171
Negative	271 (37.3%)	287 (39.5%)	
Indeterminate	7 (1%)	5 (0.7%)	
Positive	89 (12.2%)	68 (9.4%)	
PAM50, n (%)			< 0.001
Normal	12 (1.1%)	28 (2.6%)	
LumA	225 (20.8%)	337 (31.1%)	
LumB	103 (9.5%)	101 (9.3%)	
Her2	54 (5%)	28 (2.6%)	
Basal	147 (13.6%)	48 (4.4%)	
Menopause status, n (%)			0.078
Pre	111 (11.4%)	118 (12.1%)	
Peri	27 (2.8%)	13 (1.3%)	
Post	350 (36%)	353 (36.3%)	
Anatomic neoplasm subdivisions, n (%)			0.604
Left	286 (26.4%)	277 (25.6%)	
Right	255 (23.5%)	265 (24.5%)	
Radiation_therapy, n (%)			0.403
No	226 (22.9%)	208 (21.1%)	
Yes	272 (27.6%)	281 (28.5%)	
OS event, n (%)			0.921
Alive	464 (42.8%)	467 (43.1%)	
Dead	77 (7.1%)	75 (6.9%)	
DSS event, n (%)			1
Alive	490 (46.1%)	488 (45.9%)	
Dead	43 (4%)	42 (4%)	
PFI event, n (%)			0.714
Alive	465 (42.9%)	471 (43.5%)	
Dead	76 (7%)	71 (6.6%)	
Age, median (IQR)	58 (49, 68)	59 (48, 67)	0.79

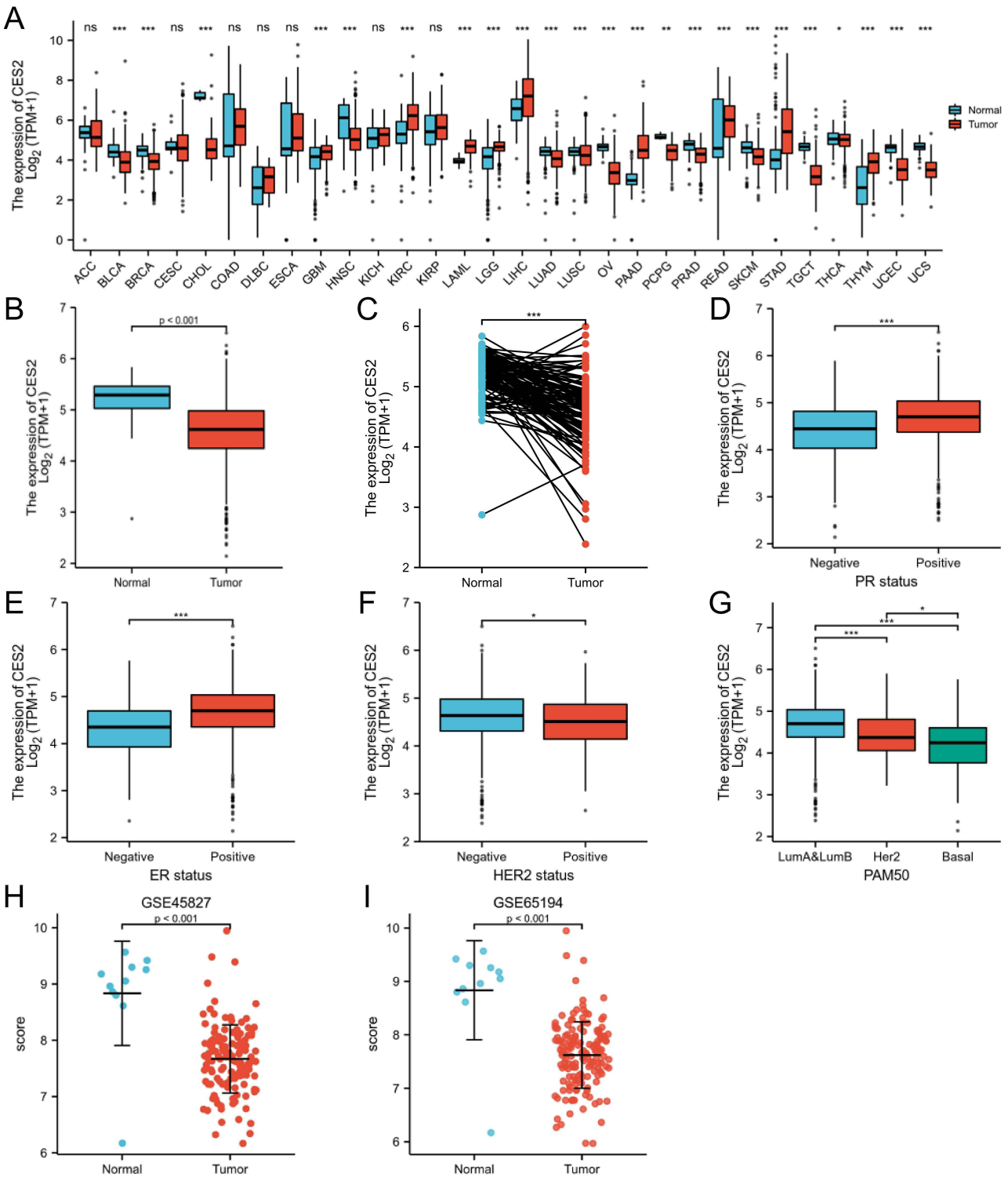

Figure 1 Expression levels of CES2 in cancer tissues. (**A**) The expression levels of CES2 in various cancer tissues differ from their corresponding normal tissues. (**B**) Expression of CES2 in unpaired tissues of breast cancer. (**C**) Expression of CES2 in paired tissues of breast cancer. (**D**–**G**) Expression of CES2 in different PR, ER, HER2 status, and PAM50 typing. (**H** and **I**) Expression of CES2 in GSE45827 and GSE65194. (*p < 0.05, ** p < 0.01, *** p < 0.001).
Abbreviation: ns, no significance.

Validation of CES2 Expression Levels in BRCA

To verify the expression of CES2, representative cell lines from several different BRCA cell types were selected for the Western blotting assay and real-time fluorescence quantitative PCR experiments of CES2. The results are shown in

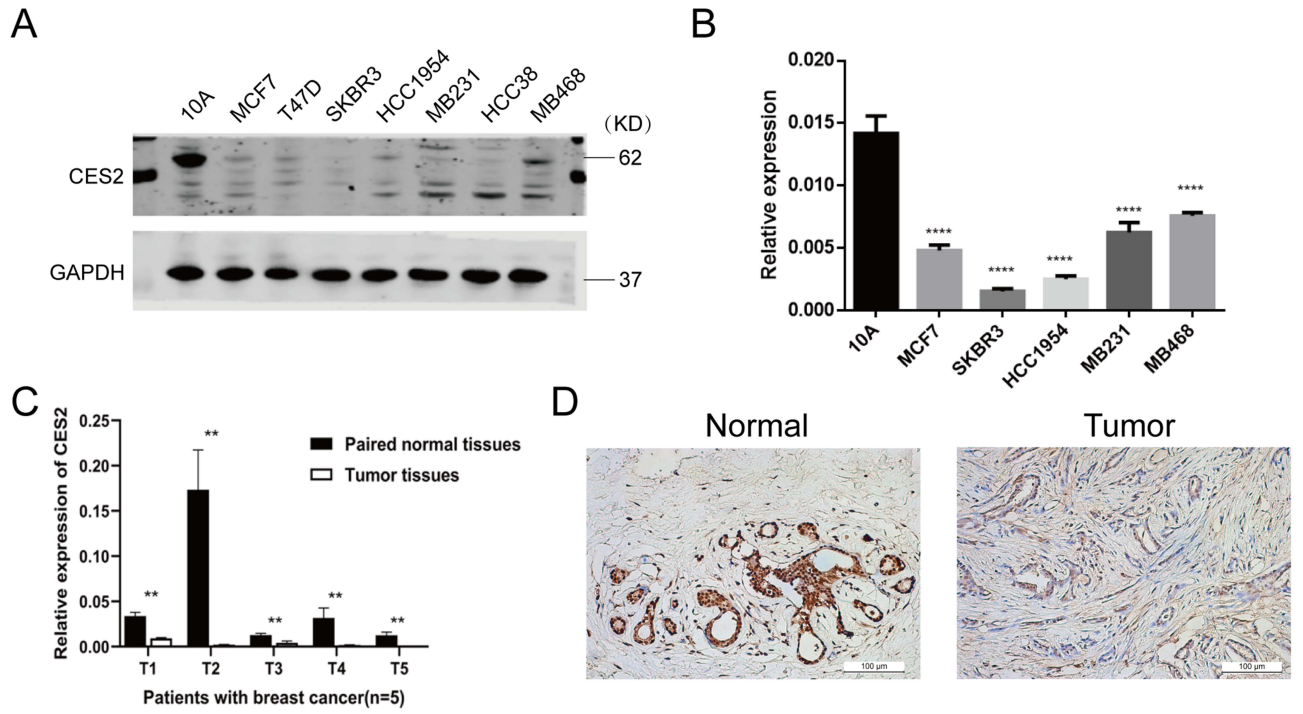

Figure 2 Validation of CES2 expression levels in breast cancer cell lines and tissues. (**A** and **B**) Expression levels of CES2 in cells were examined by Western blot assay and real-time fluorescence quantitative PCR assay. (**C**) Expression levels of CES2 in tissues were examined by real-time fluorescence quantitative PCR assay. (**D**) Expression levels of CES2 protein in tissues were examined by IHC. (**p < 0.01, ****p < 0.0001).

Figure 2A and B; the expression of CES2 in breast normal cell was much higher than that in all other BRCA cell types, and the difference was statistically significant (P < 0.01). Next, we randomly selected cancer and paracancer tissues diagnosed with BRCA for real-time fluorescence quantitative PCR experiments and found that the expression level of CES2 in normal tissues was still higher than that in cancer tissues (Figure 2C). Further analysis showed homology with IHC results (Figure 2D). Supplementary Table 1 demonstrates the basic clinicopathological characteristics of the included patients.

Prognostic Correlation Analysis

Kaplan–Meier survival curves showed that CES2 expression levels correlated with overall survival in patients with stage T4 BRCA (Figure 3A). Meanwhile, the PrognoScan database showed that high CES2 levels were associated with better relapse-free survival (RFS) in GSE12276 and better distant metastasis-free survival (DMFS) in GSE19615 (Figure S1). Receiver operating characteristic (ROC) were used to analyze the diagnostic values of CES2 in BRCA patients. The area under the ROC curve was 0.829. This result suggested that CES2 was able to distinguish between normal and tumor tissues (Figure 3B). In the following analysis, all AUC values for CES2 were greater than 0.7 in all TNM stages, invasive ductal carcinoma, and invasive lobular carcinoma, suggesting that CES2 had good diagnostic value in TNM stages, invasive ductal carcinoma, and invasive lobular carcinoma (Figure 3C).

PPI Network and Enrichment Analysis of CES2

We constructed an interaction network between CES2 and its related genes using the STRING tool. The results are shown in Figure 4. CES2-related genes included ESD, CES1, UGT1A8, UGT1A1, UGT1A6, GUSB, CYP3A4, LRAT, RBP4, and CDA, and their scores were greater than 0.8 (Figure 4A and B). We used the GO and KEGG methods to perform a preliminary analysis of the enrichment of CES2 major pathways. The results showed that the molecular functions of CES2 were mainly enriched in retinoic acid binding, isoprenoid binding, and retinoid binding. The cellular components of CES2 are mainly enriched in the cytochrome complex, the endoplasmic reticulum chaperone complex,

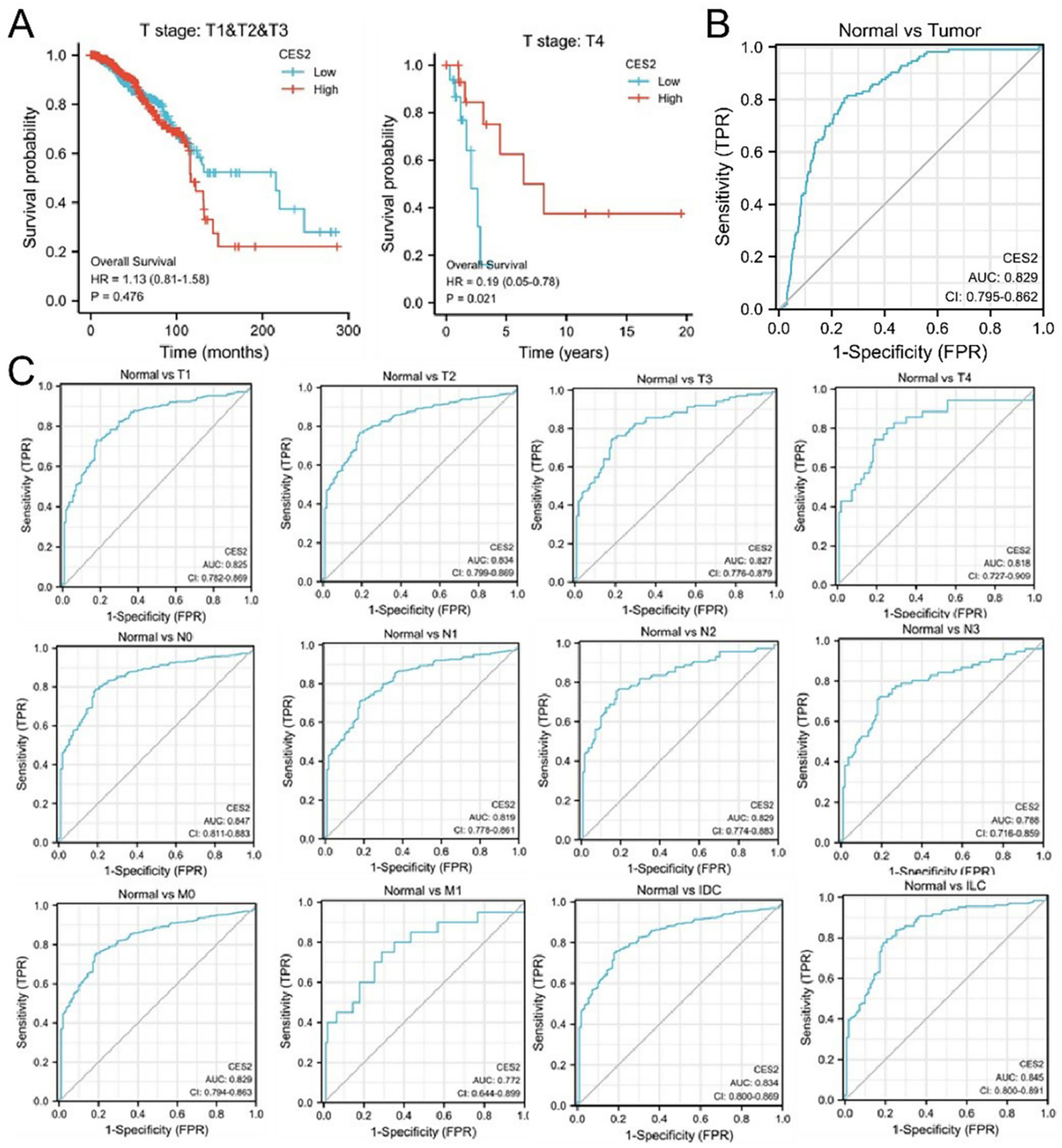

Figure 3 Kaplan–Meier survival curves and ROC analysis curves of CES2 patients. (**A**) Correlation between CES2 expression and prognosis in breast cancer stages T1, T2, T3, and T4. (**B** and **C**) Diagnostic value of ROC analysis of CES2 in all stages of TNM, invasive ductal carcinoma, and invasive lobular carcinoma.

and the endoplasmic reticulum lumen. The biological process of CES2 is mainly enriched in hormone metabolic process, cellular response to xenobiotic stimulus, and xenobiotic metabolic process. The KEGG pathway of CES2 was mainly enriched in three metabolic pathways: ascorbate and aldarate metabolism; retinol metabolism; and drug metabolism by other enzymes (Figure 4C and D). These results suggest that CES2 is mainly enriched in metabolism-related signaling pathways and plays a key role in metabolic processes.

A

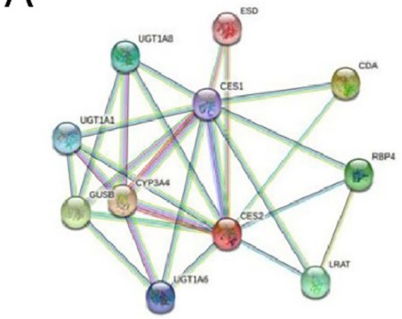

B

Gene symbol	Annotation	score
CYP3A4	Cytochrome p450 family 3 subfamily a polypeptide 4	0.951
CDA	Cytidine deaminase	0.924
GUSB	Beta-glucuronidase	0.921
RBP4	Retinol-binding protein 4	0.902
LRAT	Phosphatidylcholine-retinol o-acyltransferase	0.901
UGT1A8	UDP-glucuronosyltransferase 1-1	0.843
UGT1A1	Udp glucuronosyltransferase family 1 member a1	0.843
UGT1A6	UDP-glucuronosyltransferase 1-6	0.83
ESD	S-formylglutathione hydrolase	0.801

C

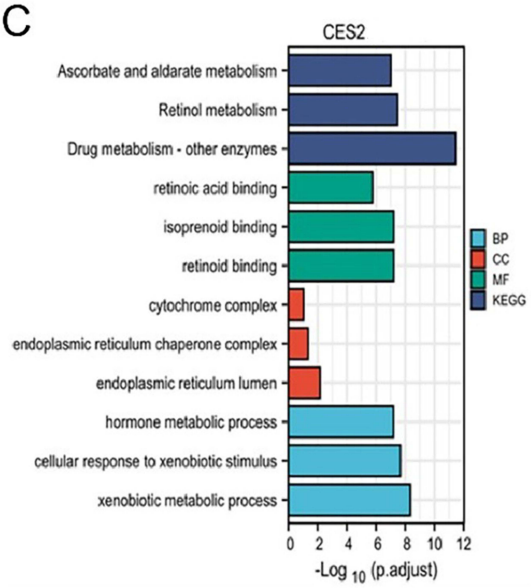

D

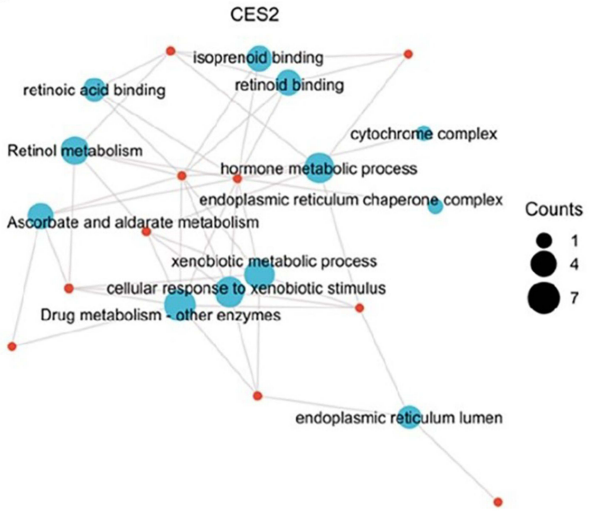

Figure 4 PPI network and enrichment analysis of CES2. (**A** and **B**) Visual bubble diagrams of the protein-protein interaction network formed by CES2 with interacting proteins, as well as details of the associated genes, analyzed using the STRING tool. (**C**) Graphical representation of the results of the CES2 molecular GO and KEGG enrichment analysis by the clusterProfiler package. (**D**) Graphical representation of the results of visualization processing of GO and KEGG enrichment analysis of CES2 molecules.

Correlation Analysis of Immune Cell Infiltration

There is growing evidence for a strong correlation between BRCA and the immune microenvironment. TIMER data showed a statistically significant association between CES2 and B cells, CD8+ T cells, CD4+ T cells, macrophages, and dendritic cells (all $p < 0.05$), while there was no statistically significant difference between neutrophils ($p > 0.05$; Figure 5A). The correlations between CES2 and other immune cells were determined using the GSVA package (Figure 5B and C). The results showed that CES2 was positively correlated with immune cells such as eosinophils, mast cells, and natural killer NK cells and negatively correlated with immune cells such as dendritic cells, Th1 cells, and Treg cells. Then, to understand the association between CES2 and immune infiltration, TISIDB was employed to evaluate the association between CES2 expression and various immune characteristics. The results also showed that CES2 correlated with a variety of tumor-infiltrating lymphocytes in breast cancer (Figure S2). This suggests that CES2 may also play a role in the immune microenvironment of BRCA.

Application of the CES2-Targeted Fluorescent Probe DDAB in BRCA

DDAB is a highly selective and sensitive near-infrared "on-off" fluorescent probe that targets CES2. In this experiment, we successfully applied the DDAB probe and first examined its cytotoxicity in a BRCA cell line, and the results showed that the DDAB probe has a low biological toxicity with low impact on overall cell survival (Figure 6A and B). The cytofluorimetric imaging results showed that the fluorescence intensity of CES2 in each BRCA cell line was significantly

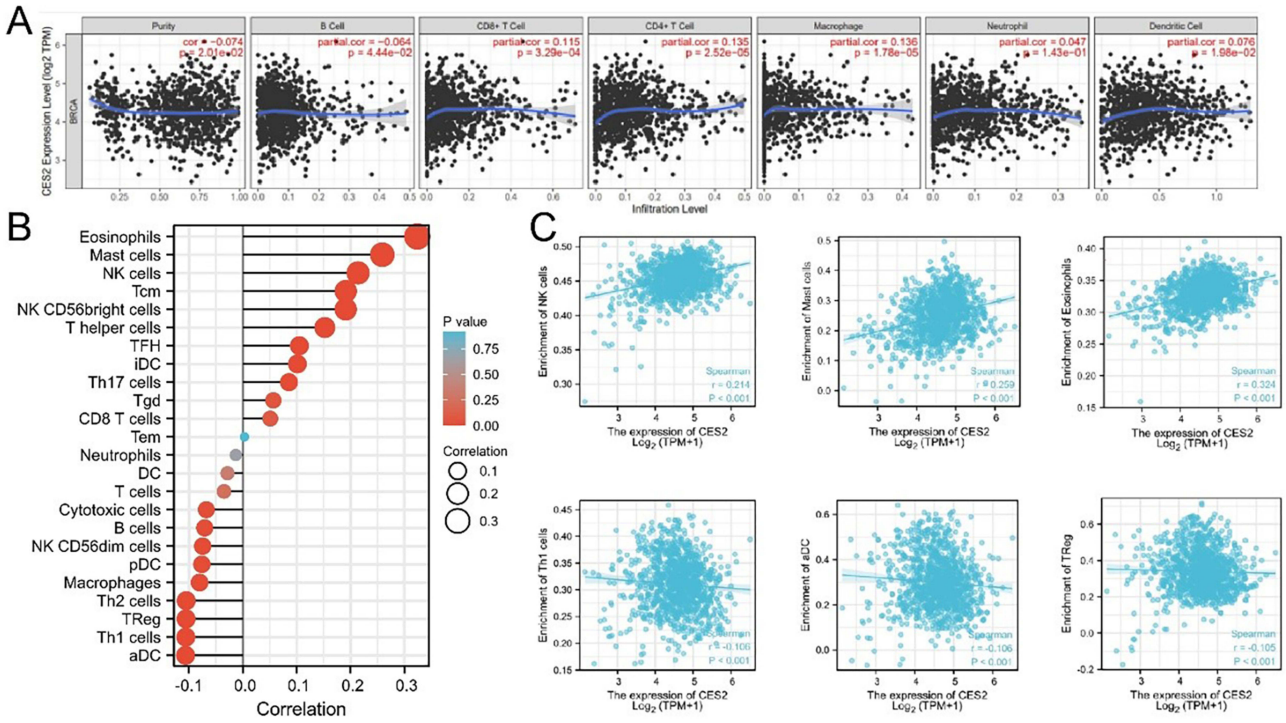

Figure 5 Correlation of CES2 expression with immune cell infiltration in breast cancer. (**A**) Analysis of the relationship between CES2 expression and tumor purity and six immune cells by TIMER database. (**B**) Lollipop plot of CES2 correlation with different immune infiltrating cells in breast cancer analyzed by GSVA package. (**C**) Correlation of CES2 with several breast cancer immune infiltrating cells was calculated by ssGSEA.

lower than that of normal breast cells, and also indicated that DDAB had better targeting performance on CES2 with excellent imaging performance (Figure 6C and E). In addition, the results of flow fluorescence analysis showed that DDAB had good labeling and sorting ability in large numbers of breast cells, and its ability to identify normal breast tissue was much greater than that of various types of BRCA cells (Figure 6D and F). In an ex vivo human tumor tissue model (Figure 6G), the DDAB probe could clearly distinguish the boundaries of the tumor from normal tissue. This demonstrates that the DDAB probe has promising applications in clinical surgery.

Discussion

CES2 plays an important role in the development of cancer. The CES2-targeting NIR fluorescent probe DDAB has low toxicity, high specificity in BRCA cells, and strong screening ability to identify cells with high CES2 expression.

BRCA is the most common malignancy among female patients, and female patients with BRCA often have the highest mortality rate.[17] The identification of new prognostic markers could provide new directions for the early detection of BRCA, reducing mortality and lowering recurrence rates. The mammalian carboxylesterase (CESs) genus is a member of the serine esterase superfamily, which is found in tissues such as the liver, intestines, lungs, and kidneys, and in cells, mainly in the endoplasmic reticulum and cytoplasm.[18] The most important physiological function of CESs is to efficiently catalyze the hydrolysis of various lipid- and amide-containing xenobiotics,[19,20] including some ester prodrugs such as clopidogrel, irinotecan ciclopirox, and oseltamivir, as well as environmental toxicants such as pyrethroids.[21,22] Recent studies have shown that CES2 plays an important role in the development of colorectal, neuroblastoma, and pancreatic cancers.[13–15] However, the molecular function of CES2 in BRCA has not been fully elucidated.

In the present study, based on bioinformatic analysis, we found significant differences between CES2 expression and clinical traits such as race, histological typing, PR, ER, and PAM50 typing. CES2 was differentially expressed in multiple cancer types and had significantly lower expression levels in invasive BRCA, which was our focus, than in normal breast tissue. Survival curve analysis showed that low CES2 expression was associated with a poor prognosis. The main CES2

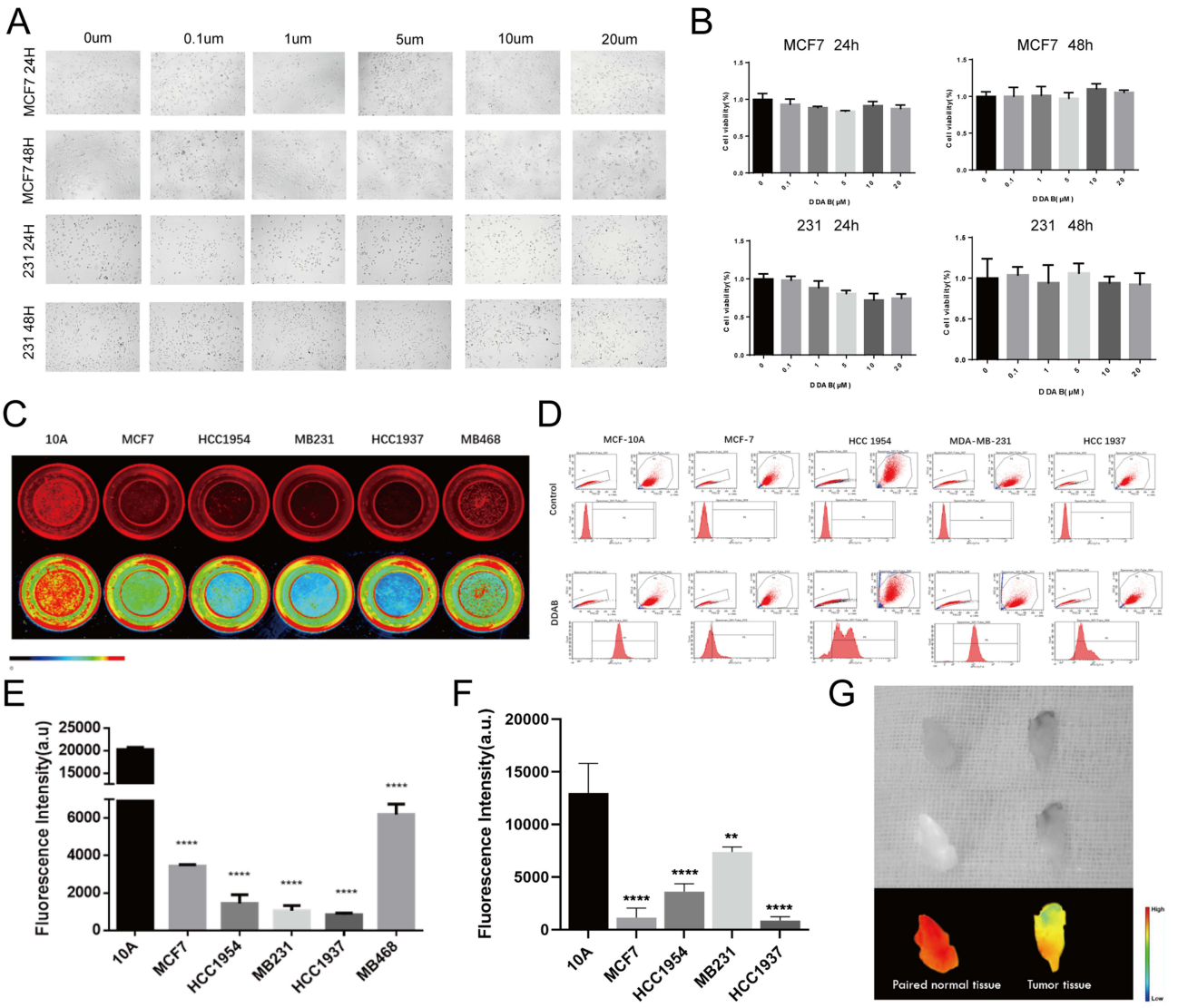

Figure 6 Validation of the efficiency of the targeted fluorescent probe DDAB. (**A** and **B**) DDAB fluorescent probe cytotoxicity assay. (**C** and **E**) Statistical plots of fluorescence imaging of DDAB probe molecules in breast cancer cells and their corresponding fluorescence values. (**D** and **F**) Flow analysis of DDAB fluorescent probe cells and their corresponding statistical plots. (**G**) Human breast cancer ex vivo tissue imaging experiments. (**p < 0.01, ****p < 0.0001).

co-expressed genes were ESD, CES1, UGT1A8, UGT1A1, UGT1A6, GUSB, CYP3A4 LRAT, RBP4, and CDA, and CES2 was mainly enriched in the metabolic pathway.

Tumor immune microenvironment has been demonstrated to be related to tumor development, progression, and drug resistance, and thus affecting the prognosis of BRCA patients.[23,24] There is an increasing awareness of the importance of immune cell infiltration in tumor progression of BRCA.[25] Our results showed a positive correlation between CES2 and immune cells, such as eosinophils, mast cells, and natural killer NK cells, and a negative correlation with immune cells, such as dendritic cells, Th1 cells, and Treg cells. Overall, our findings revealed the important role of CES2 in immune regulation in BRCA.

Additionally, fluorescence-guided cancer detection is one of the most promising methods for intraoperative assessment of surgical margins in BRCA, and the ability to obtain intraoperative "tumor-free margins" is essential for the prevention of recurrence after lumpectomy.[26,27] The CES2-targeted fluorescent probe DDAB is a DDAO-based NIR fluorescent probe with low photodamage, high tissue penetration, and low interference from background autofluorescence in complex biological systems.[16]

In this study, we detected the expression of CES2 in different BRCA cells and tissues. We also applied the CES2-targeted fluorescent probe DDAB to BRCA for the first time. We verified the low toxicity of the probe in various breast cells through various molecular experiments and its high specific targeting and "on-off" utility, which allows labeling and sorting of large numbers of breast cells. The fluorescence of DDAB can also clearly distinguish the border between tumor and normal tissues in isolated human tumor models. The above experimental results indicate that DDAB fluorescent probes may have potential for surgical oncology applications, which is worthy of further exploration to provide a theoretical and experimental basis for the early clinical translation of fluorescent probes for surgical navigation.

Conclusion

In conclusion, our study suggests that Low CES2 expression is closely associated with a worse prognosis in the BRCA T4 stage, and CES2 might contribute to the development of immunological treatment strategies. Meanwhile, CES2 is able to distinguish between breast normal and tumor tissues, the CES2-targeting NIR fluorescent probe DDAB may have potential for surgical applications in BRCA.

Acknowledgments

This work was supported by the Guidance Plan of the Natural Science Foundation of Liaoning Province (No. 2019-ZD -0927).

Disclosure

The authors report no conflicts of interest in this work.

References

1. Sung H, Ferlay J, Siegel RL, et al. Global cancer statistics 2020: GLOBOCAN estimates of incidence and mortality worldwide for 36 cancers in 185 countries. *CA*. 2021;71(3):209–249. doi:10.3322/caac.21660
2. Harbeck N, Penault-Llorca F, Cortes J, et al. Breast cancer. *Nat Rev Dis Primers*. 2019;5(1):66. doi:10.1038/s41572-019-0111-2
3. Hamann M, Grill S, Struck J, et al. Detection of early breast cancer beyond mammographic screening: a promising biomarker panel. *Biomark Med*. 2019;13(13):1107–1117. doi:10.2217/bmm-2019-0085
4. Mayor S. Screening for early breast cancer reduces invasive cancer, study finds. *BMJ*. 2015;351:h6576. doi:10.1136/bmj.h6576
5. Wang D, Zou L, Jin Q, Hou J, Ge G, Yang L. Human carboxylesterases: a comprehensive review. *Acta Pharm Sin B*. 2018;8(5):699–712. doi:10.1016/j.apsb.2018.05.005
6. Zhu HJ, Wang X, Gawronski BE, Brinda BJ, Angiolillo DJ, Markowitz JS. Carboxylesterase 1 as a determinant of clopidogrel metabolism and activation. *J Pharmacol Exp Ther*. 2013;344(3):665–672. doi:10.1124/jpet.112.201640
7. Imai T, Ohura K. The role of intestinal carboxylesterase in the oral absorption of prodrugs. *Curr Drug Metab*. 2010;11(9):793–805. doi:10.2174/138920010794328904
8. Nishi K, Huang H, Kamita SG, Kim IH, Morisseau C, Hammock BD. Characterization of pyrethroid hydrolysis by the human liver carboxylesterases hCE-1 and hCE-2. *Arch Biochem Biophys*. 2006;445(1):115–123. doi:10.1016/j.abb.2005.11.005
9. Zhu HJ, Markowitz JS. Activation of the antiviral prodrug oseltamivir is impaired by two newly identified carboxylesterase 1 variants. *Drug Metab Dispos*. 2009;37(2):264–267. doi:10.1124/dmd.108.024943
10. Walko CM, Lindley C. Capecitabine: a review. *Clin Ther*. 2005;27(1):23–44. doi:10.1016/j.clinthera.2005.01.005
11. Pratt SE, Durland-Busbice S, Shepard RL, Heinz-Taheny K, Iversen PW, Dantzig AH. Human carboxylesterase-2 hydrolyzes the prodrug of gemcitabine (LY2334737) and confers prodrug sensitivity to cancer cells. *Clin Cancer Res*. 2013;19(5):1159–1168. doi:10.1158/1078-0432.ccr-12-1184
12. Hatfield MJ, Tsurkan L, Garrett M, et al. Organ-specific carboxylesterase profiling identifies the small intestine and kidney as major contributors of activation of the anticancer prodrug CPT-11. *Biochem Pharmacol*. 2011;81(1):24–31. doi:10.1016/j.bcp.2010.09.001
13. Zhang Y, Sun L, Sun Y, et al. Overexpressed CES2 has prognostic value in CRC and knockdown CES2 reverses L-OHP-resistance in CRC cells by inhibition of the PI3K signaling pathway. *Exp Cell Res*. 2020;389(1):111856. doi:10.1016/j.yexcr.2020.111856
14. Uchida K, Otake K, Tanaka K, et al. Clinical implications of CES2 RNA expression in neuroblastoma. *J Pediatr Surg*. 2013;48(3):502–509. doi:10.1016/j.jpedsurg.2012.10.004
15. Chen Y, Capello M, Rios Perez MV, et al. CES2 sustains HNF4α expression to promote pancreatic adenocarcinoma progression through an epoxide hydrolase-dependent regulatory loop. *Mol Metab*. 2022;56:101426. doi:10.1016/j.molmet.2021.101426
16. Jin Q, Feng L, Wang DD, et al. A highly selective near-infrared fluorescent probe for carboxylesterase 2 and its bioimaging applications in living cells and animals. *Biosens Bioelectron*. 2016;83:193–199. doi:10.1016/j.bios.2016.04.075
17. Bray F, Ferlay J, Soerjomataram I, Siegel RL, Torre LA, Jemal A. Global cancer statistics 2018: GLOBOCAN estimates of incidence and mortality worldwide for 36 cancers in 185 countries. *CA*. 2018;68(6):394–424. doi:10.3322/caac.21492
18. Satoh T, Hosokawa M. Structure, function and regulation of carboxylesterases. *Chem Biol Interact*. 2006;162(3):195–211. doi:10.1016/j.cbi.2006.07.001
19. Zhang C, Xu Y, Zhong Q, et al. In vitro evaluation of the inhibitory potential of pharmaceutical excipients on human carboxylesterase 1A and 2. *PLoS One*. 2014;9(4):e93819. doi:10.1371/journal.pone.0093819

20. Liu D, Gao J, Zhang C, Ren X, Liu Y, Xu Y. Identification of carboxylesterases expressed in rat intestine and effects of their hydrolyzing activity in predicting first-pass metabolism of ester prodrugs. *Die Pharmazie*. 2011;66(11):888–893.
21. Crow JA, Borazjani A, Potter PM, Ross MK. Hydrolysis of pyrethroids by human and rat tissues: examination of intestinal, liver and serum carboxylesterases. *Toxicol Appl Pharmacol*. 2007;221(1):1–12. doi:10.1016/j.taap.2007.03.002
22. Xu Y, Zhang C, He W, Liu D. Regulations of xenobiotics and endobiotics on carboxylesterases: a comprehensive review. *Eur J Drug Metab Pharmacokinet*. 2016;41(4):321–330. doi:10.1007/s13318-016-0326-5
23. Burugu S, Asleh-Aburaya K, Nielsen TO. Immune infiltrates in the breast cancer microenvironment: detection, characterization and clinical implication. *Breast Cancer*. 2017;24(1):3–15. doi:10.1007/s12282-016-0698-z
24. Lee KH, Kim EY, Yun JS, et al. The prognostic and predictive value of tumor-infiltrating lymphocytes and hematologic parameters in patients with breast cancer. *BMC Cancer*. 2018;18(1):938. doi:10.1186/s12885-018-4832-5
25. Xu Q, Chen S, Hu Y, Huang W. Landscape of immune microenvironment under immune cell infiltration pattern in breast cancer. *Front Immunol*. 2021;12:711433. doi:10.3389/fimmu.2021.711433
26. Dintzis SM, Hansen S, Harrington KM, et al. Real-time visualization of breast carcinoma in pathology specimens from patients receiving fluorescent tumor-marking agent tozuleristide. *Arch Pathol Lab Med*. 2019;143(9):1076–1083. doi:10.5858/arpa.2018-0197-OA
27. Lu G, van den Berg NS, Martin BA, et al. Tumour-specific fluorescence-guided surgery for pancreatic cancer using panitumumab-IRDye800CW: a Phase 1 single-centre, open-label, single-arm, dose-escalation study. *Lancet Gastroenterol Hepatol*. 2020;5(8):753–764. doi:10.1016/s2468-1253(20)30088-1